Title
Hepatic GATA4 regulates cholesterol and triglyceride homeostasis in collaboration with LXRs

Journal
Genes & Development, 36(21-24)

ISSN
0890-9369

Authors
Bideyan, Lara
López Rodríguez, Maykel
Priest, Christina
et al.

Publication Date
2022-11-01

DOI
10.1101/gad.350145.122

Peer reviewed

Hepatic GATA4 regulates cholesterol and triglyceride homeostasis in collaboration with LXRs

Lara Bideyan,[1,2] Maykel López Rodríguez,[1,2] Christina Priest,[1,2] John P. Kennelly,[1,2] Yajing Gao,[1,2] Alessandra Ferrari,[1,2] Prashant Rajbhandari,[1,2] An-Chieh Feng,[3] Sergei G. Tevosian,[4] Stephen T. Smale,[3] and Peter Tontonoz[1,2]

[1]Department of Pathology and Laboratory Medicine, University of California at Los Angeles, Los Angeles, USA; [2]Department of Biological Chemistry, University of California, Los Angeles, Los Angeles, USA; [3]Department of Microbiology, Immunology, and Molecular Genetics, University of California at Los Angeles, Los Angeles, USA; [4]Department of Physiological Sciences, University of Florida, Gainesville, Florida 32610, USA

GATA4 is a transcription factor known for its crucial role in the development of many tissues, including the liver; however, its role in adult liver metabolism is unknown. Here, using high-throughput sequencing technologies, we identified GATA4 as a transcriptional regulator of metabolism in the liver. GATA4 expression is elevated in response to refeeding, and its occupancy is increased at enhancers of genes linked to fatty acid and lipoprotein metabolism. Knocking out GATA4 in the adult liver (Gata4LKO) decreased transcriptional activity at GATA4 binding sites, especially during feeding. Gata4LKO mice have reduced plasma HDL cholesterol and increased liver triglyceride levels. The expression of a panel of GATA4 binding genes involved in hepatic cholesterol export and triglyceride hydrolysis was down-regulated in Gata4LKO mice. We further demonstrate that GATA4 collaborates with LXR nuclear receptors in the liver. GATA4 and LXRs share a number of binding sites, and GATA4 was required for the full transcriptional response to LXR activation. Collectively, these results show that hepatic GATA4 contributes to the transcriptional control of hepatic and systemic lipid homeostasis.

[*Keywords*: LXR; lipid metabolism; transcription factor]

Supplemental material is available for this article.

Received October 1, 2022; revised version accepted December 2, 2022.

The liver plays a vital role in systemic lipid and glucose metabolism (Rui 2014). The liver is the major site for synthesis of lipids and lipoproteins. It converts excess dietary carbohydrates and proteins into lipids during feeding and maintains glucose homeostasis through gluconeogenesis during fasting. Dysregulation of hepatic metabolism is central to the development of nonalcoholic fatty liver diseases (NAFLDs), insulin resistance, and atherosclerosis (Goldstein and Brown 2015; Duell et al. 2022). Dissection of the transcriptional landscape in physiological responses such as fasting and feeding is needed to expand our understanding of metabolic regulatory networks and their vulnerabilities in pathologies.

GATA4 is a zinc finger protein belonging to GATA family of transcription factors. While GATA1–3 are expressed in the hematopoietic system and central nervous system, GATA4–6 are expressed in endoderm- and mesoderm-derived tissues such as the heart, liver, pancreas, and gonads (Lentjes et al. 2016). GATA4 is known to play an essential role in the development of many of these tissues and in cardiac hypertrophy (Molkentin et al. 1997; Oka et al. 2006). Global knockout of GATA4 is embryonic-lethal due to heart and liver agenesis (Molkentin et al. 1997; Watt et al. 2007), making studies of adult tissues challenging. In the liver, GATA4 has been reported to be involved in hepatocyte differentiation and to serve as a tumor suppressor gene (Enane et al. 2017). GATA4 activity in stellate cells has been tied to quiescence and the prevention of liver fibrosis (Arroyo et al. 2021). The action of GATA4 in liver sinusoidal endothelial cells (LSECs), but not in hepatocytes, appears to be important for liver regeneration (Zheng et al. 2013; Winkler et al. 2021). However, the role of GATA4 in transcriptional regulation in adult hepatocytes is poorly understood.

GATA4 is a pioneer factor that binds predominantly to enhancer regions and is capable of opening closed

Corresponding author: ptontonoz@mednet.ucla.edu
Article published online ahead of print. Article and publication date are online at http://www.genesdev.org/cgi/doi/10.1101/gad.350145.122.

chromatin (Romano and Miccio 2020). GATA4 binding to its target genes is tissue-specific, in part due to its interactions with other transcription factors. While it is capable of both activating and repressing gene expression, prior studies suggest that in the liver, GATA4 functions primarily as an activator (Zheng et al. 2013). GATA4 is known to recruit the transcriptional activator p300 to chromatin, where it increases the acetylation of histone H3 on lysine 27 (H3K27ac) and enhancer activity (He et al. 2014).

In addition to its roles in differentiation and identity maintenance, GATA4 has been associated with metabolism. Genetic studies in humans have found association of GATA4 with plasma triglycerides (TGs) and with type 2 diabetes (T2D) (Lamina et al. 2011; Asselbergs et al. 2012; Ding et al. 2021; Chou et al. 2022). Other reports have suggested that GATA4 regulates steroidogenesis and glycolysis in Leydig cells (Bergeron et al. 2015; Schrade et al. 2015) and that loss of intestinal GATA4 prevents diet-induced obesity (Patankar et al. 2011). However, the metabolic consequences of hepatocyte-specific loss of GATA4 in adult mice are unknown.

In this study, we used integrated transcriptional and epigenetic analyses to characterize GATA4 as a regulator of the feeding response in the adult liver. We show that loss of GATA4 alters the hepatic transcriptional landscape during feeding, reduces plasma HDL cholesterol levels, and increases liver triglyceride accumulation. Finally, we demonstrate that GATA4 cooperates with LXR in the regulation of genes linked to cholesterol homeostasis.

Results

GATA4 activity and expression are up-regulated in response to feeding

To investigate changes in the hepatic transcriptional landscape during feeding, we conducted ATAC-seq and RNA-seq on livers of mice fasted for 12 h and those of mice fasted and then refed for 12 h with high-sucrose diet. We adapted the time points and diet from previously published protocols to maximize the insulin and lipogenic response (Liang et al. 2002). Based on the chromatin accessibility profiled via ATAC-seq, we inferred genomic regions that were changing in activity during feeding. We identified 3314 differentially accessible peaks, with 1231 gaining accessibility in fasted conditions and 2083 gaining accessibility in refed conditions (Fig. 1A). The differentially accessible peaks in the fasted and refed states were primarily located in intergenic and intronic regions, followed by promoter regions (Fig. 1B). Annotating peaks to the closest promoter led to the observation that peaks more accessible in fasting were associated with genes involved in the PPAR signaling pathway (Supplemental Fig. S1A) and that peaks more accessible in refeeding were associated with fatty acid biosynthesis, ChREBP activation, and other pathways (Supplemental Fig. S1B). These associations strongly suggested that the dynamic changes in the chromatin that we observed in response to fasting and refeeding were linked to transcriptional changes known to regulate these metabolic processes (Bideyan et al. 2021).

We next sought to identify transcription factors that might have differential activity in these two states. We analyzed how the prevalence of different transcription factor binding motifs changed across all peaks in relation to the change in accessibility in those peaks between fasting and refeeding. The peaks were ranked by fold change and grouped into bins. We then ran motif enrichment analysis for each of these motifs on each bin and plotted the *P*-values (Fig. 1C). Motifs for transcription factors known to be involved in fasting, such as those for PPARα, glucocorticoid receptor (GR), and FOXO1, were enriched in bins more accessible in fasting livers. Similarly, motifs for factors known to be involved in feeding, such as those for SREBP1, C/EBP, and JUN, were enriched in peaks more accessible in refed livers. Interestingly, the GATA family motif was enriched in peaks more accessible during refeeding, compared with peaks similarly or more accessible during fasting (Fig. 1C; Supplemental Fig. S1C). In the refed condition, the average accessibility of peaks with the GATA4 motif within the top 10 bins was >50% higher in refed than in fasted mice (Fig. 1D). This finding was unexpected, as GATA family proteins were not previously known to be involved in the feeding response. The peaks with higher accessibility in refeeding that also had GATA family motifs clustered separately from those with motifs for other transcription factors, defining a unique signal and activity pattern for the GATA family in the refeeding response (Supplemental Fig. S1D). Peaks with increased GATA family motif accessibility in refed livers were associated with genes linked to lipid, lipoprotein, and fatty acid metabolism, including *Srebf1*, *Insig1*, *Apoa1*, *Gpam*, *Pnpla3*, *Acsl5*, *Acaca*, *Fabp1*, *Elovl5*, and others (Fig 1E). Further analysis showed enrichment of the C/EBPα motif among refed peaks with GATA motifs (P-value = 1×10^{-205}), suggesting possible collaboration between C/EBPα and GATA proteins in the feeding response (Supplemental Fig. S1E).

In addition to using the binning approach, we validated the increase in the accessibility of the GATA4 motif in the refed condition by testing it on differentially accessible peaks in fasted and refed conditions. Among the 3314 differentially accessible peaks, 424 had GATA4 motifs with an enrichment P-value of 1×10^{-19}. Among peaks with higher accessibility in the refed condition, 297 were enriched for the GATA4 motif, while among peaks with higher accessibility in the fasted condition, 127 were enriched for the GATA4 motif. The enrichment of the GATA4 motif had a P-value of 1×10^{-18} among the peaks with increased accessibility in the refeeding condition and a P-value of 1×10^{-3} among the peaks with increased accessibility in the fasting condition. While the frequency of peaks with the GATA4 motif among not differentially accessible regions was 8.45%, the frequency was 14.26% for the peaks with increased accessibility in the refeeding condition and 10.32% for the ones with increased accessibility in the fasting condition.

RNA-seq showed that, among the GATA family, only transcripts for *Gata4* and *Gata6* were expressed in the

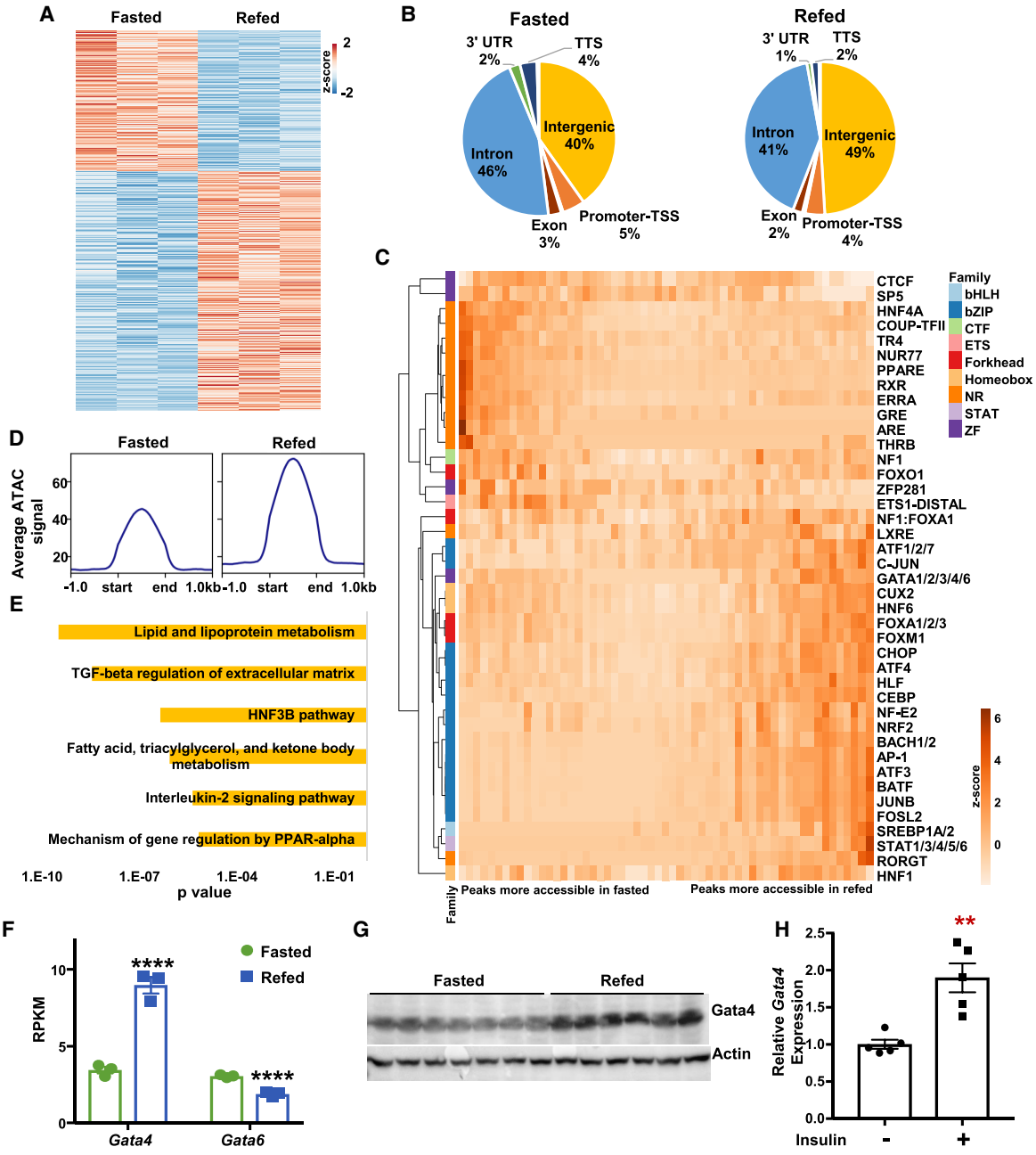

Figure 1. GATA4 motif accessibility and expression is up-regulated in liver by feeding. (*A*,*B*) Heat map (*A*) and genomic features (*B*) of 3314 differentially accessible ATAC-seq peaks in fasted versus refed livers. One-thousand-thirty-one peaks were differentially more accessible in the fasted condition and 2083 peaks were more accessible in the refed condition. (*C*) Hierarchical clustering heat map for transcription factor motif enrichment across all ATAC-seq peaks, ranked and binned (~1000 peaks/bin) based on the accessibility fold change between fasted and refed livers. The motif enrichment for selected transcription factor families is plotted. (*D*) Average accessibility profile at sites with GATA4 motif among the top 10 bins more accessible in refed livers. (*E*) Pathway enrichment analysis of genes associated with peaks in *D*. (*F*) RPKM of GATA family members detected by RNA-seq. (*G*) Western blot analysis of GATA4 protein expression in fasted and refed livers. (*H*) qPCR analysis of *Gata4* expression in Hepa1–6 cells treated with DMEM without glucose or glutamine and with or without 100 nM insulin for 8 h. Data are expressed as mean ± SEM. Statistical analysis was performed using two-tailed Student's *t*-test with comparisons made between each group and its respective control. (**) $P < 0.01$, (****) $P < 0.001$. (NR) Nuclear receptors, (ZF) zinc finger.

liver (Fig. 1F). Gene expression of other transcription factors from Figure 1C is shown in Supplemental Figure S2A. *Gata4* was more abundant than *Gata6*, and its levels increased approximately twofold in response to refeeding. In contrast, *Gata6* decreased in the refeeding condition, making GATA4 the most likely mediator of the increased GATA family activity seen in our ATAC-seq analysis. Additionally, we validated the up-regulation of *Gata4*

transcript and protein levels by qPCR and by Western blotting (Fig. 1G; Supplemental Fig. S2B–D). Analysis of publicly available RNA-seq data comparing ad libitum fed mice versus 24-h-fasted mice (Kinouchi et al. 2018) showed that circadian regulation of *Gata4* is dependent on feeding (Supplemental Fig. S2E). We further determined that insulin was the likely cause of the *Gata4* up-regulation during feeding. In Hepa1–6 cells, treatment with insulin resulted in similar up-regulation of *Gata4* expression (Fig. 1H). Based on these observations, we hypothesized that GATA4 plays a role in the hepatic metabolic response to feeding.

Loss of GATA4 alters the hepatic feeding response

Since GATA4 is essential for liver development (Watt et al. 2007), we knocked out GATA4 in livers of *Gata4*-floxed adult mice by administration of a hepatocyte-specific AAV8-Cre vector (Gata4LKO mice). qPCR analysis of fasted and refed mice 1 wk after injection showed up to an 83% reduction in *Gata4* expression in mice receiving AAV8-Cre compared with vector controls (Fig. 2A). Since liver endothelial and stellate cells are also known to express *Gata4* (Winkler et al. 2021), residual *Gata4* expression was expected. This remaining *Gata4* expression was not responsive to feeding.

Metabolic phenotyping revealed that Gata4LKO mice had lower plasma cholesterol levels in both fasted and refed conditions (Fig. 2B), implying that GATA4 might have a role in cholesterol homeostasis independent of the feeding response. Fast protein liquid chromatography (FPLC) fractionation of plasma from refed mice showed decreased HDL cholesterol levels in Gata4LKO samples compared with controls (Fig. 2C). Plasma triglycerides (TGs) and nonesterified fatty acids (NEFA) were not different between groups (Supplemental Fig. S3A,B). Liver cholesterol was increased in Gata4LKO mice in the fasted state (Fig. 2D), suggesting a possible defect in cholesterol transport from the liver to plasma. Fasted liver TGs trended higher in Gata4LKO samples compared with controls (Fig. 2E), while liver glycogen was reduced in refed Gata4LKO mice (Fig. 2F).

Lipidomic analysis revealed feeding-specific effects of loss of hepatic GATA4 on glycerophospholipids and ceramides. Liver ceramides were decreased in refed control samples in comparison with fasted controls (Fig. 2G,H). However, this refeeding-induced reduction in liver ceramides was impaired in Gata4LKO mice. Liver ceramide

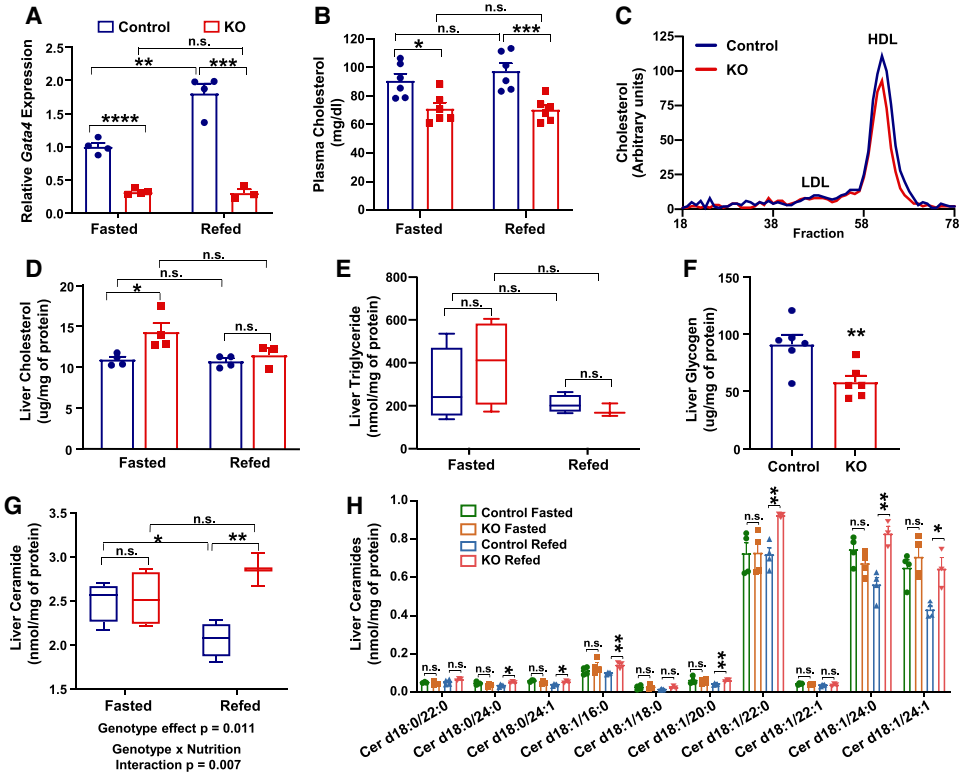

Figure 2. Loss of *Gata4* in the liver alters the hepatic and systemic lipid profile in fasting and in feeding conditions. Seven days to 10 d after AAV injection, Gata4LKO and control mice were either fasted (12 h) or fasted (12 h) and then refed with HS diet for 12 h. (*A*) qPCR assessment of *Gata4* expression. (*B*) Plasma total cholesterol measurement. (*C*) Total cholesterol level in FPLC fractionated plasma. Plasma from four to five mice was pooled for each group. (*D*) Liver total cholesterol. (*E*) Lipidomic analysis of liver triglycerides (TGs) ($n = 3$–4). (*F*) Liver glycogen in refed Gata4LKO versus control mice. Total (*G*) and individual species (*H*) of liver ceramides from the lipidomics analysis in *E*. Data in bar plots are expressed as mean ± SEM, and data in box plots are expressed as minimum to maximum. Statistical analysis was performed using two-tailed Student's *t*-test with comparisons made between each group and its respective control (*A*–*H*) and two-way ANOVA for the effects of genotype and nutrition (*G*). (*) $P < 0.05$, (**) $P < 0.01$, (***) $P < 0.001$, (n.s.) not significant.

levels were higher in refed Gata4LKO mice in comparison with refed control mice, and there was a statistically significant interaction between genotype and feeding status. Among phospholipids, phosphatidylglycerol (PG) and phosphatidylcholine (PC) species trended higher in refed Gata4LKO mice, while phosphatidylethanolamines were unchanged (Supplemental Fig. S3C–E). Last, liver FA and sphingomyelin levels were increased in Gata4LKO mice across nutritional states (Supplemental Fig. S2F,G). Overall, our phenotypic analysis demonstrated that loss of hepatic GATA4 altered phospholipid and ceramide metabolism during feeding, and cholesterol metabolism in both the fasted and fed states.

GATA4 transcriptional targets in fasted and refed livers

We next conducted RNA-seq and H3K27ac ChIP-seq on control and Gata4LKO livers from mice fasted or refed with a high-sucrose diet. Principal component analysis and hierarchical clustering showed clustering of replicates and separation of knockout from control samples in each condition for both RNA-seq and H3K27ac ChIP-seq (Supplemental Fig. S4A–C). Both methods showed greater separation between knockout and control samples in the refed condition. Using RNA-seq, we confirmed an 82% reduction in the reads from excised exons of the *Gata4* gene (Supplemental Fig. S4D).

The RNA-seq data revealed genes differentially expressed between Gata4LKO and control livers during fasting or feeding (Supplemental Fig. S4E). Down-regulated genes in Gata4LKO mice were enriched for those linked to "lipid and lipoprotein metabolism," "lipid mobilization," and "HDL-mediated lipid transport" (Fig. 3A). These included genes involved with cholesterol efflux, such as *Apoa1*, *Apoa2*, *Abcg5*, *Abcg8*, *Abca1*, *Alb*, and *Soat2*, and genes with lipid binding and lipid hydrolase functions, such as *Fabp2*, *Ces2a*, *Ces3b*, *Ces2g*, *Lipc*, and *Lipa* (Fig. 3B). Many of these genes were down-regulated in both fasted and refed conditions (Fig. 3C). We also performed gene set enrichment analysis (GSEA) by ranking all genes based on their fold change and *P*-value in refed Gata4LKO mice and controls. GSEA independently showed down-regulation of the cholesterol efflux pathway in Gata4LKO mice (Fig. 3D). The finding of reduced plasma HDL cholesterol in Gata4LKO mice is consistent with reduced cholesterol efflux from the liver (Fig. 2B,C).

Genes relating to FA and glycerophospholipid metabolism were down-regulated in Gata4LKO compared with control mice, specifically in the refed condition (Fig. 3B). Integrated pathway analysis (IPA) determined the "SREBP1 pathway" to be down-regulated in refed Gata4LKO mice based on the down-regulation of the *Srebf1* gene and SREBP1c target genes such as *Gpam*, *Pnpla3*, and *Acyl* in refed Gata4LKO mice (Supplemental Fig. S4F). Moreover, genes that were only down-regulated in refed Gata4LKO mice were enriched for the "glycerophospholipid metabolism pathway" and included *Pcyt2*, *Pgs1*, *Pisd*, and *Pla2g12b* (Fig. 3B,C). The refed-specific changes in this pathway were consistent with increases observed in glycerophospholipids in Gata4LKO mice (Supplemental Fig. S3C–E). Genes relating to ceramide metabolism were down-regulated in refed Gata4LKO mice, especially *Sgpl1*, which encodes the protein that performs the last step in ceramide degradation (Fig. 3B). Reduction of *Sgpl1* expression was consistent with the increased ceramide levels seen in refed Gata4LKO livers (Fig. 2G,H). Using publicly available GATA4 liver ChIP-seq data (GSE49131), we determined that many of these down-regulated genes involved in cholesterol and sphingomyelin metabolism and SREBP signaling had GATA4 binding sites within or proximal to the gene body, making them likely to be direct targets of GATA4 (Supplemental Fig. S4G).

In fasting mice, we observed that SREBP2 and its targets in the cholesterol biosynthesis pathway were strongly down-regulated in Gata4LKO livers compared with controls (Fig. 3B,C). Cholesterol inhibits its own biosynthesis by down-regulating the SREBP2 targets (Yang et al. 2002). The increased cholesterol levels in fasted Gata4LKO livers were therefore in line with the down-regulation of cholesterol synthesis genes (Fig. 2D).

In contrast to the down-regulation of many genes linked to lipid metabolism genes, genes relating to glucose metabolism and gluconeogenesis pathways were up-regulated in Gata4LKO livers compared with controls (Fig. 3E). In particular, qPCR analysis confirmed that the gene for the rate-limiting enzyme for gluconeogenesis, PEPCK (*Pck1*), had higher expression in refed Gata4LKO mice (Supplemental Fig. S4H). Increased gluconeogenesis would be consistent with the reduced glycogen levels observed in Gata4LKO livers (Fig. 2F). Overall, these results indicate complementary shifts in both lipid metabolism and glucose metabolism in the absence of GATA4.

Loss of GATA4 reduces transcriptional activity at GATA4 binding sites

H3K27ac is a marker of active enhancers and promoters (Creyghton et al. 2010). By performing H3K27ac ChIP-seq on the same livers used for RNA-seq, we assessed activity in regulatory regions in relation to transcriptional changes in Gata4LKO mice in both fasted and refed conditions. We analyzed the H3K27ac changes near GATA4 binding sites from GATA4 liver ChIP-seq (GSE49131) and observed an average decrease in transcriptional activity at GATA4 binding regions in both fasted and refed Gata4LKO livers (Fig. 4A). We used publicly available H3K4me1 ChIP-seq (GSM722760) and H3K4me3 ChIP-seq (GSM722761) from livers as additional markers for enhancers and promoters. Out of 5867 GATA4 ChIP-seq peaks, 1735 were within 1 kb of the enhancer marker H3K4me1, and 1711 were within 1 kb of the promoter marker H3K4me3. The GATA4 peaks associated with enhancers and promoters lost H3K27ac enrichment in Gata4LKO livers (Fig. 4B).

We identified GATA4 binding regions with differential H3K27ac enrichment in Gata4LKO and control livers (Fig. 4C). While 209 regions were differentially enriched in Gata4LKO livers only in the refed condition, 90 were differentially enriched only in the fasted condition, and 56

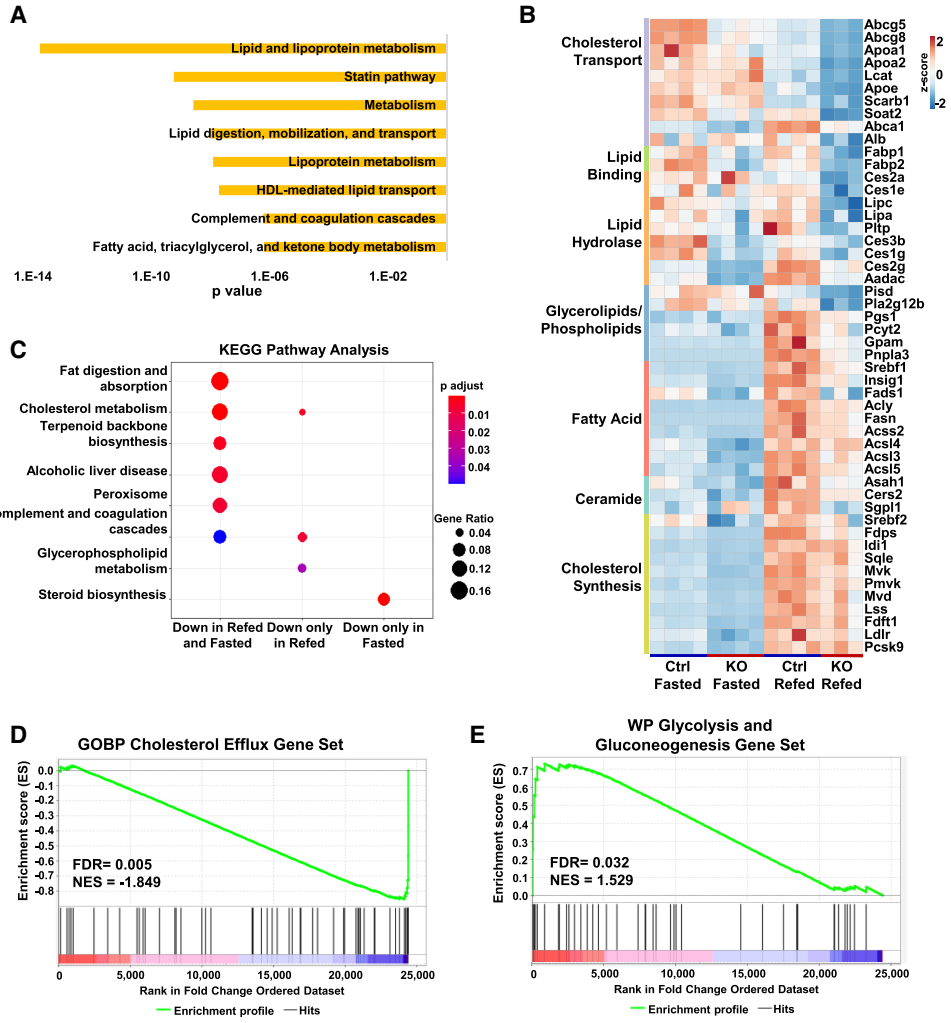

Figure 3. Loss of *Gata4* down-regulates lipid metabolism pathways in fasting and in feeding conditions. RNA-seq of Gata4LKO and control liver samples fasted for 12 h or refed for 12 h with HS diet after 12 h fasting. (*A*) Bioplanet pathway enrichment analysis of down-regulated genes in refed Gata4LKO liver RNA-seq compared with refed control livers. (*B*) Heat map of the expression of selected genes involved in the indicated metabolic processes, which are down-regulated in fasted or refed Gata4LKO livers compared with their respective controls. (*C*) KEGG pathway enrichment analysis of down-regulated genes in Gata4LKO livers in only the fasted or refed conditions or in both. (*D*,*E*) Gene set enrichment analysis (GSEA) of the GO biological pathway cholesterol efflux pathway (*D*) and the Wikipathways glycolysis and gluconeogenesis gene set (*E*) among all expressed genes ranked for their fold change and *P*-value in Gata4LKO versus control livers in the refed condition.

were differentially enriched in both conditions. A majority of the differentially regulated GATA4 binding regions lost enhancer activity in Gata4LKO livers, and the magnitude of loss was greater in the refed state (Fig. 4D). To further address whether GATA4 was required for changes in transcriptional activity during feeding, we analyzed H3K27ac signal in the regions of ATAC peaks with increased GATA family motif accessibility in refed livers. The average level of H3K27ac near these peaks was greater in refed controls than in fasted controls. Moreover, the increase in activity during feeding was blunted in Gata4LKO liver (Fig. 4E). For instance, candidate Gata4 sites associated with the feeding-induced genes *Pnpla3*, *Acsl5*, *Srebf1*, and others lost enhancer activity in refed Gata4LKO livers, while the GATA4 binding site at its canonical target gene, *Zfpm1*, lost activity in Gata4LKO livers in both conditions (Fig. 4F; Supplemental Fig. S5A).

We also looked at the H3K27ac signal at the *Gata4* gene to gain insight into the regulation of *Gata4* expression. While there are H3K27ac peaks that had stronger enrichment in the control refed condition compared with the control fasted condition, for many of them this increase was attenuated in the Gata4LKO livers, indicating that GATA4 binding at these locations at least partially was responsible for the transcriptional activity. However, we identified two intronic regions in which the increase in H3K27ac enrichment due to refeeding remains even in the absence of GATA4 (Supplemental Fig. S5B). These sites overlapped with a modest increase in average ATAC-seq signal in refed WT mice compared with fasted

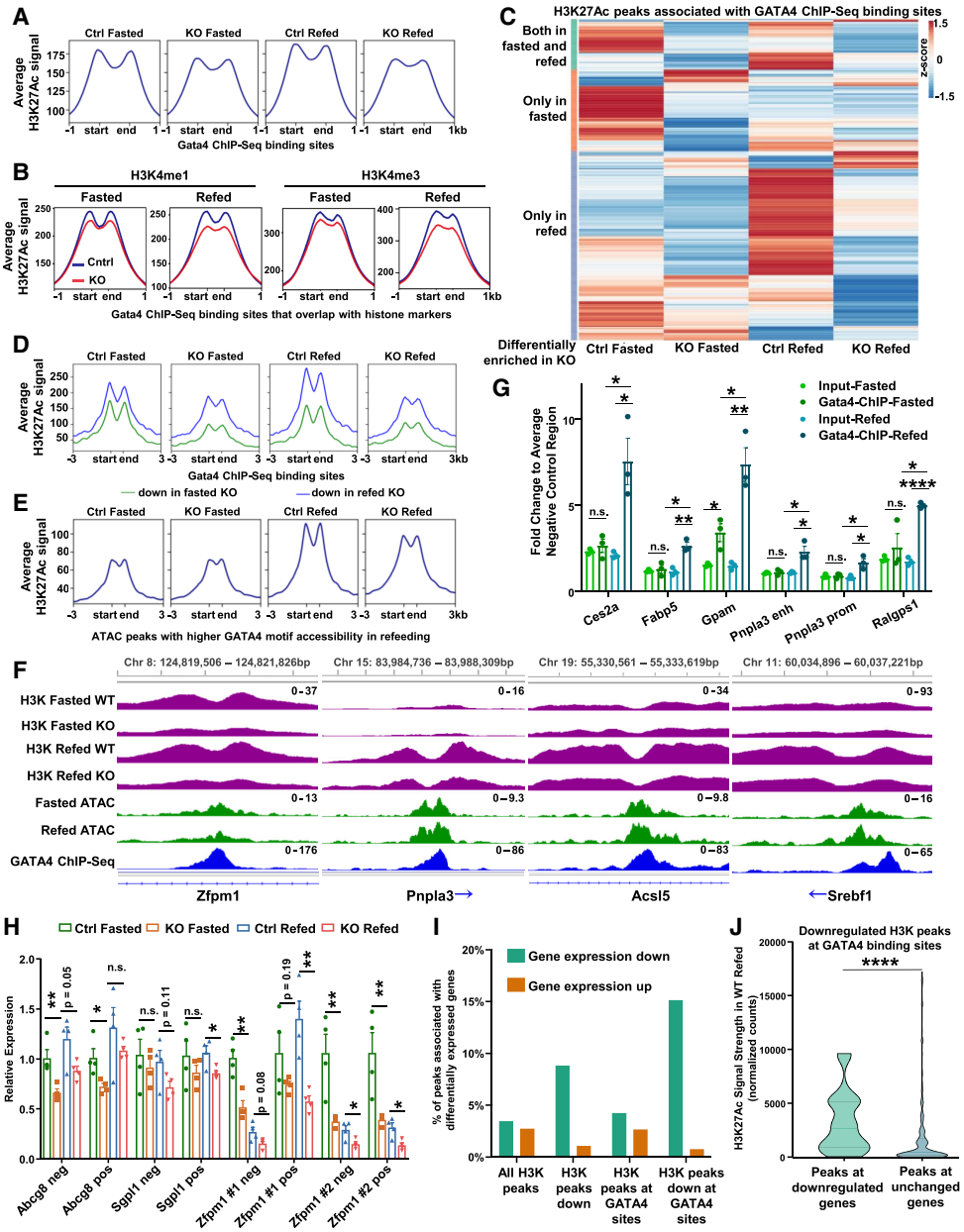

Figure 4. GATA4 has common and differential targets in fasted versus refed livers. (*A*) Profile of H3K27ac ChIP-seq signal within 1 kb of GATA4 ChIP-seq binding sites (GSE49131). (*B*) Profile of H3K27ac ChIP-seq signal at GATA4 ChIP-seq binding sites that were within 1 kb of H3K4me1 (*left*) or H3K4me3 (*right*) peaks from the liver (GSE29218). (*C*,*D*) Heat map of 355 H3K27ac ChIP-seq peaks (*C*) and profile of H3K27ac ChIP-seq signal (*D*) within 500 bp of GATA4 ChIP-seq binding sites that were differentially enriched in Gata4LKO compared with control mice in fasted or refed conditions. (*E*) H3K27ac profile at regions identified from ATAC-seq with GATA4 motifs among the top 10 bins that were more accessible in refed livers. (*F*) Example IGV view of H3K27ac ChIP-seq of GATA4LKO and control livers in both refed and fasted conditions. ATAC-seq of wild-type refed and fasted livers and GATA4 ChIP-seq at GATA4 targets. The regions are annotated to the gene with the closest promoter. Tick marks are 500 bp apart. (*G*) GATA4 ChIP-qPCR of selected candidate regions for increased GATA4 binding in refed samples. The bar graph shows values for target regions of both the input and ChIP samples that were normalized to the average of two negative control regions within each sample. Data are expressed as mean ± SEM. Statistical analysis was performed by two-tailed *t*-tests between ChIP samples from fasted and refed states or between each group and its respective control. (*H*) qPCR assessment of eRNAs of selected regions in fasted and refed controls versus Gata4LKO livers. "pos" and "neg" refer to the transcripts on the positive and the negative strands, respectively. (*I*) Percentage of H3K27ac peaks that were proximal to differentially expressed genes in refed Gata4LKO mice compared with controls, based on adjacency (500 bp) to GATA4 binding sites or differential H3K27ac enrichment in refed Gata4LKO mice. (*J*) H3K27ac peaks adjacent to GATA4 binding sites that are down-regulated in KO refed mice were selected. They were separated into groups based on changes in the expression of the closest gene in KO refed mice. The WT refed H3K27ac signal of these groups is plotted. K-S test was performed for statistical analysis. (*) $P < 0.05$, (**) $P < 0.01$, (****) $P < 0.0001$, (n.s.) not significant.

WT mice. These sites have been reported to be bound by a number of transcription factors in the liver, including LXRs, RXRα, C/EBPα, HNF4α, STAT5α, and FOXA1/2. One or a combination of these transcription factors may be partially responsible for inducing Gata4 expression during feeding.

We validated the differential binding of GATA4 at some of these sites by conducting ChIP-qPCR on the same liver samples (Fig. 4G). GATA binding sequences from *Ces2a*, *Fabp5*, *Gpam*, *Pnpla3*, and *Ralgps1* were enriched in GATA4 ChIP samples from refed compared with fasted livers, indicating increased binding of GATA4 with feeding at these regions. Additionally, for select GATA4 binding sites, we confirmed that the absence of GATA4 reduced the enhancer RNA (eRNA) expression at those locations, some in the fasted or refed condition only and some in both conditions (Fig. 4H). Overall, our data show that GATA4 binding can be affected by nutritional state and can impact H3K27ac levels and eRNA transcription at its target enhancers.

Integrating H3K27ac activity with the Gata4LKO RNA-seq and GATA4 ChIP-seq data, we sought to understand the factors that correlated with changes in gene expression. We asked whether GATA4 binding or H3K27ac at a GATA4 binding site was predictive of its differential expression of the cognate gene between WT and Gata4LKO mice. Indeed, the strength and change in H3K27ac signal and GATA4 binding were strongly associated with down-regulated genes (Fig. 4I,J; Supplemental Fig. S5C).

To assess how other transcription factors were responding to the loss of hepatic GATA4, we analyzed transcription factor motif enrichment at sites of changing H3K27 acetylation. As expected, the GATA motif was enriched in regions with decreased H3K27 acetylation in refed Gata4LKO livers (Supplemental Fig. S5D). Interestingly, binding motifs for two key transcription factors involved in the fasting response, PPARα and FOXO1, were enriched in regions with increased H3K27 acetylation in refed Gata4LKO livers (Supplemental Fig. S5E). This suggests inadequate suppression of fasting responses in refed Gata4LKO livers. We further conducted pathway analysis on the genes associated with regions of differential H3K27 acetylation in refed Gata4LKO livers. Regions with decreased H3K27 acetylation were enriched for genes associated with the AKT and insulin signaling pathways (Supplemental Fig. S5F). Regions with increased H3K27 acetylation were enriched for genes associated with AMPK signaling (Supplemental Fig. S4G). For some of these genes, including *Srebf1* and *Pck1*, changes in H3K27 acetylation mirrored changes in gene expression (Fig. 3B; Supplemental Fig. S4H), providing further evidence for disruption of the feeding response in Gata4LKO livers.

Loss of hepatic GATA4 leads to TG accumulation in the liver

Based on the observation that loss of GATA4 altered the expression of some hepatic genes regardless of feeding status, we explored potential metabolic functions for GATA4 beyond our fasting and refeeding paradigm. We hypothesized that increasing the TG and cholesterol content in their diet might provoke additional phenotypes in Gata4LKO mice. We fed mice chow or Western diet (WD) for 3–4 wk after AAV injection and sacrificed them after 6 h of fasting. Plasma cholesterol levels were lower in Gata4LKO mice compared with controls on both chow and WD (Fig. 5A). Liver cholesterol levels were modestly increased in Gata4LKO mice only in the chow-fed condition (Fig. 5B). On both chow and WD, liver TGs more than doubled in Gata4LKO mice (Fig. 5C). Hematoxylin and eosin (H&E) and Oil Red O staining of liver sections from WD-fed mice confirmed hepatic lipid accumulation in Gata4LKO mice (Fig. 5D; Supplemental Fig. S6A). Lipidomic analysis of chow-fed liver samples showed that liver TGs with diverse fatty acid content were broadly increased (Fig. 5E). On both chow and WD, liver fatty acids were also elevated in Gata4LKO mice compared with controls (Supplemental Fig. S6B). Liver glycogens were reduced in Gata4LKO, especially on WD (Supplemental Fig. S6C). There was no difference in VLDL secretion (Supplemental Fig. S6D).

We analyzed gene expression to further characterize the phenotype of Gata4LKO mice on WD. Data from RNA-seq of Gata4LKO and control mice after 3 wk on WD clustered by genotype (Supplemental Fig. S7A) and revealed 716 genes down-regulated and 1029 up-regulated in Gata4LKO livers (Supplemental Fig. S7B). Expression of genes linked to cholesterol metabolism, including transport genes such as *ApoA1*, *Apoc1*, *Abcg5*, and *Abcg8*, was reduced in WD-fed Gata4LKO mice (Fig. 5F). Many of these genes were also differentially expressed in chow-fed control and Gata4LKO livers (Supplemental Fig. S7C). Moreover, fatty acid biosynthesis genes such as *Srebf1*, *Acly*, *Acaca*, and *Acsl3* showed reduced expression in WD-fed Gata4LKO mice (Fig. 5F). Given the reduction in gene expression linked to FA biosynthesis, increased lipid synthesis was unlikely to be the cause of the TG accumulation in Gata4LKO livers. We therefore assessed the expression of genes involved in FA oxidation. PPARα targets such as *Acox1*, *Ehhadh*, and others were up-regulated in Gata4LKO mice (Fig. 5G; Supplemental Fig. S7D). This pattern suggested that PPARα was activated in Gata4LKO livers secondary to hepatic TG accumulation. Interestingly, the expression of genes relating to TG hydrolysis, including *LipC*, *Ces2a*, *Aadac*, and *Ces1g*, was reduced in Gata4LKO mice, suggesting a possible mechanism for the hepatic TG accumulation (Fig. 5H). Additionally, genes linked to lipid and lipoprotein uptake, such as *Lpl*, *Cd36*, and *Vldlr*, were up-regulated in Gata4LKO mice, suggesting that increased lipid uptake may also contribute to hepatic lipid accumulation (Fig. 5G).

GATA4 collaborates with LXR to induce their joint transcriptional targets

Many of the genes down-regulated in Gata4LKO mice, including *Abca1*, *Abcg5*, *Abcg8*, *Srebf1*, and *Fasn*, are LXR targets (Repa et al. 2000a,b, 2002; Joseph et al. 2002). IPA

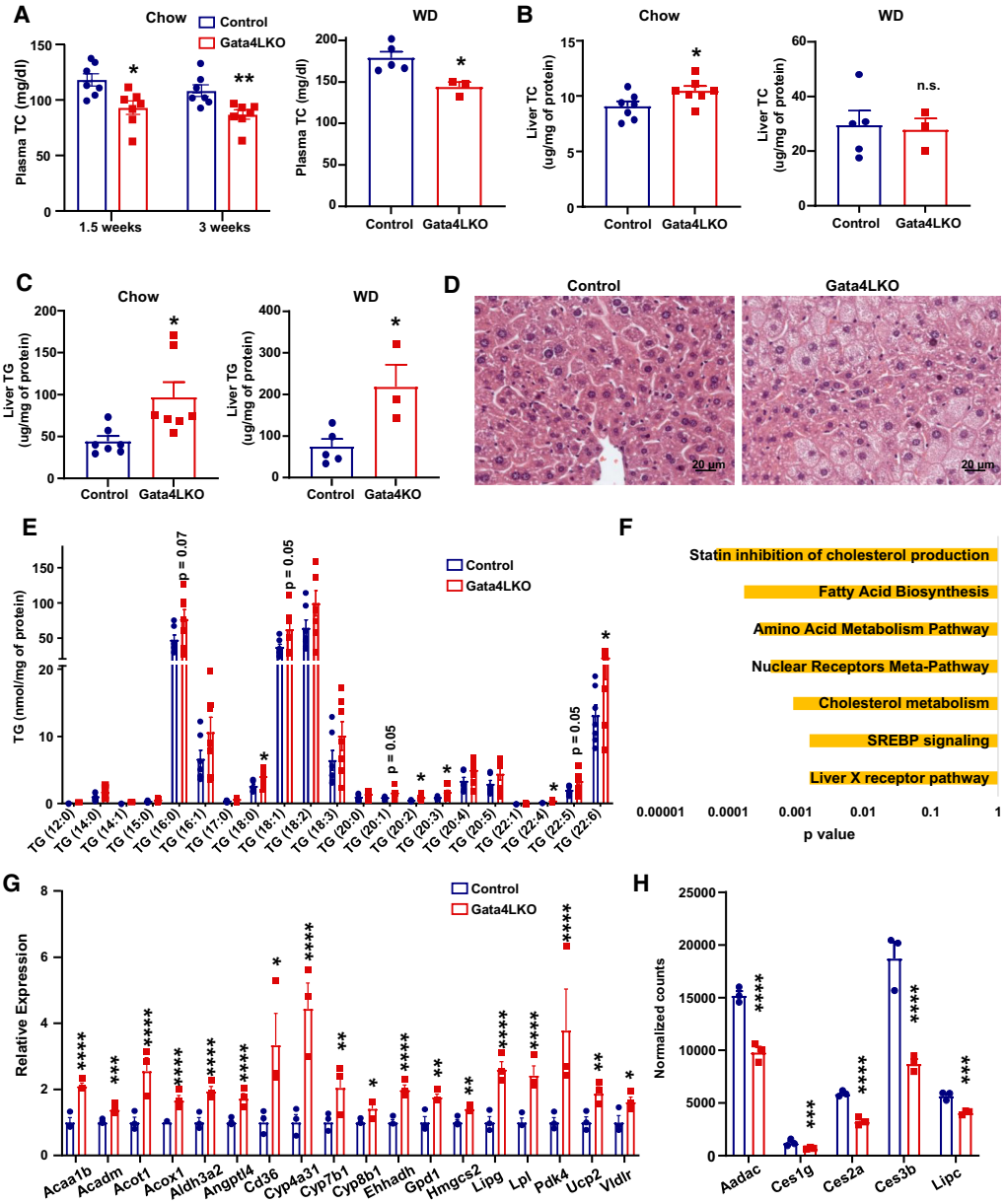

Figure 5. Loss of *Gata4* results in reduction in plasma cholesterol and accumulation of liver triglycerides. (*A–C*) Plasma total cholesterol (*A*), liver total cholesterol (*B*), and liver triglycerides (*C*) of Gata4LKO and control mice after 3 wk on chow (*left*) or Western diet (*right*). (*D*) H&E staining of Gata4 and control liver sections after 4 wk of Western diet feeding. (*E*) Lipidomics analysis of triglycerides summarized based on the fatty acyl tail content of livers of Gata4LKO and control mice on chow for 3 wk after AAV injection. RNA-seq was performed on livers of Gata4LKO versus control mice after 3 wk of Western diet treatment. (*F*) Pathway enrichment analysis of down-regulated genes in Gata4LKO livers. (*G*) Relative expression of up-regulated PPARα target genes. (*H*) Normalized counts of down-regulated genes involved in the triglyceride degradation pathway. For all panels, mice were euthanized after fasting for 6 h. Data are expressed as mean ± SEM. Statistical analysis was performed using two-tailed Student's *t*-test with comparisons made between each group and its respective control (*A–C,E*), and Wald test followed by correction for multiple testing using Benjamini and Hochberg method (*F–H*). (*) $P < 0.05$, (**) $P < 0.01$, (***) $P < 0.001$, (****) $P < 0.0001$, (n.s.) not significant.

predicted that LXRα transcriptional activity was down-regulated in Gata4LKO livers ($P = 1.02 \times 10^{-6}$) (Fig. 6A). ChIP enrichment analysis (ChEA) showed that down-regulated genes in Gata4LKO mice (fasted, refed, or WD-fed) were enriched for LXR ChIP-seq targets (Fig. 6B; Boergesen et al. 2012). Moreover, LXR ChIP-seq showed the LXR cistrome was enriched for GATA4 binding sites, especially when mice were treated with the LXR agonist T0901317, suggesting common binding of the two transcription factors (Fig. 6C). GATA4–LXR cobinding regions were associated with genes involved in lipid and lipoprotein metabolism and lipid transport (Supplemental Fig. S8A).

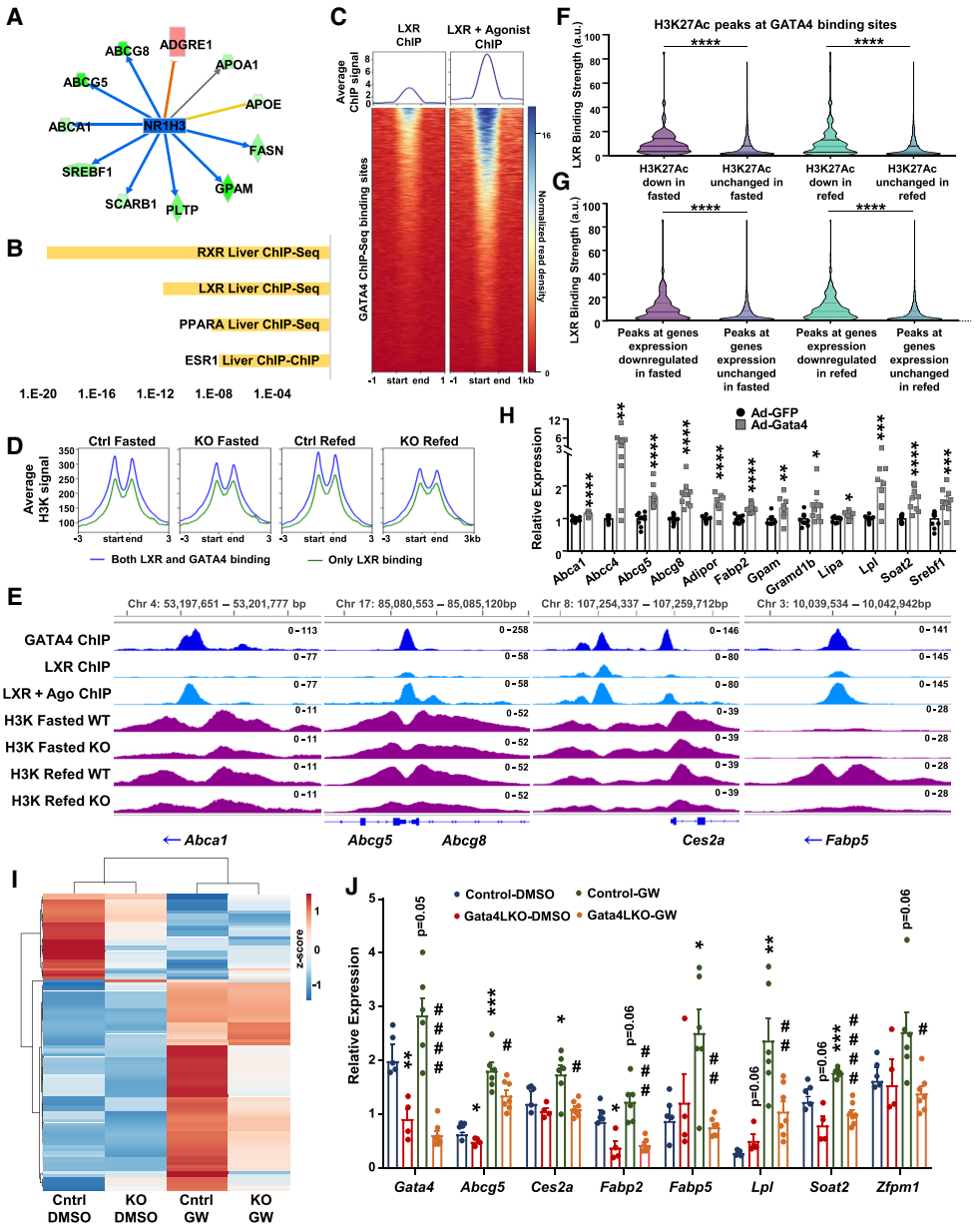

Figure 6. GATA4 collaborates with LXR to induce shared transcriptional targets. (*A*) IPA summary of the LXRα pathway in Gata4LKO RNA-seq. Green indicates down-regulated targets and red indicates up-regulated targets in refed Gata4LKO livers in contrast to controls. Blue shows predicted down-regulation of activity. (*B*) ChIP enrichment analysis (ChEA) of the down-regulated genes in RNA-seq of Gata4LKO versus control livers after 3 wk of Western diet treatment as described in Figure 5. (*C*) Profile (*top*) and heat map (*bottom*) of signal from LXR ChIP-seq with vehicle or LXR agonist T0901317 treatment (GSE35262) at 5867 GATA4 ChIP-seq sites. (*D*) Profile of signal from H3K27ac ChIP-seq from fasted and refed control and Gata4LKO samples at LXR ChIP-seq sites (with T0901317 treatment) based on whether it is within 500 bp of a GATA4 binding site (GSE49131). (*E*) IGV view of GATA4 ChIP-seq, LXR ChIP-seq with and without agonist treatment, and H3K27ac ChIP-seq of GATA4LKO and control livers in both refed and fasted conditions at example regions for common LXR and GATA4 targets. The regions are annotated to the gene with the closest promoter. (*F*,*G*) Tick marks are 1 kb apart. H3K27ac peaks adjacent to GATA4 binding sites are grouped based on either changes in H3K27ac enrichment (*F*) or changes in the expression of the closest gene with KO (*G*). LXR binding strength at these H3K27ac peaks are plotted. K-S test was performed for statistical analysis. (*H*) qPCR assessment of expression of selected LXR target genes in the livers of mice overexpressing *Gata4* or *Gfp* as control. (*I*) Gata4LKO and control mice were gavaged twice with 40 mg/kg LXR agonist GW3965 versus vehicle control DMSO. RNA-seq heat map of 104 LXR targets of this experiment. LXR targets were defined by LXR ChIP-seq targets (GSM864669) that were differentially expressed with GW3965 treatment in this experiment. (*J*) qPCR assessment of selected genes that showed a significant interaction between genotype and LXR agonist treatment effect using two-way ANOVA. Data are expressed as mean ± SEM. Statistical analysis was performed using two-tailed Student's *t*-test and two-way ANOVA for interaction between the effects of genotype and agonist treatment. (*) Comparison with control-DMSO, (#) comparison with control-GW. (*/#) $P < 0.05$, (**/##) $P < 0.01$, (***/###) $P < 0.001$, (****/####) $P < 0.0001$.

LXR and GATA4 cobinding regions were associated with changes in enhancer and transcriptional activity in Gata4LKO livers. Regions with both LXR and GATA4 binding sites on average lost H3K27ac enrichment in Gata4LKO livers (Fig. 6D). Examples of LXR and GATA4 cobinding genes include *Abca1*, *Abcg5*, *Abcg8*, *Ces2a*, and *Fabp5*. Each of these had reduced expression and H3K27 acetylation at the LXR–GATA4 binding regions in Gata4LKO livers compared with controls (Figs. 3B, 6E). Globally, a strong LXR binding signal at a GATA4 binding site was predictive of the down-regulation of H3K27ac level of that site and transcript level of the cognate gene in Gata4LKO livers (Fig. 6F,G). Additionally, we overexpressed *Gata4* mRNA in livers of adult mice using an adenoviral vector. Using qPCR, we found that many of the LXR target genes that were down-regulated in Gata4LKO mice were up-regulated in Gata4-overexpressing mice (Adeno-Gata4) versus controls (Adeno-Gfp) (Fig. 6H).

To further assess the role of GATA4 in hepatic LXR signaling, we treated control and Gata4LKO mice with the LXR agonist GW3965. We analyzed the changes in gene expression in LXR targets, defined by LXR ChIP-seq peak (GSM864669) and differential expression in response to this GW3965 treatment. The majority of these genes had a diminished response to the LXR agonist treatment in the absence of GATA4 (Fig. 6I). qPCR analysis also showed a panel of genes whose expression showed a significant interaction between genotype and LXR agonist treatment, including *Abcg5*, *Ces2a*, *Fabp2*, *Fabp5*, and *Soat2* (Fig. 6J). Induction of these genes by LXR agonist was blunted in Gata4LKO livers. We noted other genes whose expression was reduced in Gata4LKO livers at baseline but not after treatment with LXR agonist treatment, including *ApoA5*, *Insig2*, and *Scarb1* (Supplemental Fig. S8B). The expression of certain genes involved in glucose metabolism, such as *G6pc*, *Pck1*, and *Pfkfb1*, also showed interaction between Gata4LKO genotype and LXR agonist treatment, indicating that the LXR–GATA4 collaboration was not limited to cholesterol and triglyceride metabolism (Supplemental Fig. S8C).

GATA4 is associated with human LDL and HDL cholesterol levels

To address whether GATA4 was associated with hepatic metabolism in humans, we probed the Type 2 Diabetes Knowledge Portal for associations between GATA4 and human metabolic traits from combined GWASs. We found SNPs within a linkage disequilibrium (LD) block containing GATA4 that were associated with LDL and HDL cholesterol (P-value $< 5 \times 10^{8}$) (Supplemental Table S1). The top SNPs in this LD block for both phenotypes were within intronic regions of the *GATA4* gene (Supplemental Fig. S9).

Discussion

Here we used ATAC-seq to profile transcription factor motifs associated with genome-wide changes in chromatin accessibility in response to feeding. This approach led to the identification of GATA4 as a transcriptional regulator of liver metabolism during feeding. Expression of GATA4 is induced in response to insulin, GATA4 binding to certain targets is increased in response to feeding, and GATA4 binding is associated with transcriptional activity at the enhancers of a battery of genes linked to lipid metabolism. In line with an important role in liver physiology, deletion of GATA4 from adult mouse livers altered plasma and hepatic lipid levels. Our analysis also revealed that GATA4 cooperates with the nuclear receptor LXR in the regulation of cholesterol metabolic genes in the liver. These results identify GATA4 as an important transcriptional modulator of hepatic lipid homeostasis.

By deleting GATA4 via Cre-mediated recombination in adult livers, we assessed the impact of loss of GATA4 on global hepatic gene expression. GATA4 binding sites in both enhancers (marked with H3K4me1) and promoters (marked with H3K4me3) on average lost transcriptional (as reflected by H3K27ac) activity. eRNA levels were reduced by the loss of hepatic GATA4 at certain GATA4 binding sites. However, we noted that some but not all GATA4 binding sites lost transcriptional activity in Gata4LKO mice. Moreover, as seen in other studies (He et al. 2014), GATA4 target regions that lost H3K27 acetylation upon GATA4 deletion were more likely to be associated with reduced gene expression. Additionally, the strength of GATA4 binding and the H3K27ac level were predictive of whether a given GATA4 binding site was functional. This suggests that the local epigenetic context influences the impact of GATA4 binding on transcriptional activity.

Our integrated genome-wide analyses revealed at least two discrete functions for GATA4 in hepatic gene expression. One is to promote the expression of genes linked to fatty acid, phospholipid, and ceramide metabolism during feeding. A cadre of genes in these pathways had GATA4 binding motifs with increased ATAC accessibility during feeding in our analysis. Deletion of GATA4 compromised the expression of these genes specifically in refed livers. In particular, the SREBP1c pathway, a key mediator of insulin signaling, was down-regulated in refed Gata4LKO livers. GATA4's collaboration with LXR may contribute to its effects on the SREBP1 pathway, since LXR is necessary for maximum expression of SREBP1c and several of its target genes in response to feeding (Repa et al. 2000a; Joseph et al. 2002). The observation of differential gene expression based on the nutritional state of the Gata4LKO mice was supported by the finding of differential binding of GATA4 to certain sites by ChIP-qPCR. However, future studies with GATA4 ChIP-seq in the fasted and refed states would provide additional insight into how GATA4 targets vary with nutritional status.

A second function for GATA4 in the liver is to regulate a different set of genes independent of feeding status. Most prominent in this group of targets are those linked to cholesterol metabolism. Accordingly, mice lacking GATA4 in the liver had reduced plasma HDL cholesterol and

increased liver cholesterol levels. A number of key genes in cholesterol efflux, including *Apoa1*, *Abca1*, *Abcg5*, and *Abcg8*, were down-regulated in Gata4LKO livers; these may contribute to the HDL phenotype. ABCA1 mediates cholesterol transport from cells to Apo-AI, which is the major protein component of HDL (Francis 2016). LXR induces cholesterol efflux by up-regulating some of these same genes (Venkateswaran et al. 2000). It is likely that the disruption of the GATA4–LXR collaboration causes a reduction in cholesterol efflux from Gata4LKO livers. A previous study suggested that the loss of GATA4 in the jejunum reduced dietary cholesterol absorption, supporting GATA4's ability to impact cholesterol transport (Battle et al. 2008).

Liver triglycerides accumulated over time in Gata4LKO mice, and the high fat content of a WD exacerbated this accumulation. This finding is consistent with a prior study showing that GATA4 knockdown caused TG accumulation in HepG2 cells treated with oleic acid (Chou et al. 2022). Evidence from gene expression and functional assays argue against possible defects in VLDL secretion or fatty acid oxidation or an increase in fatty acid biosynthesis as the causes of hepatic lipid accumulation in Gata4LKO mice. Rather, a number of triglyceride hydrolysis genes (including *Lipc*) were down-regulated and genes involved in FA and TG uptake (such as *Lpl*) were up-regulated in Gata4LKO mice. Many members of the *Ces* family, including *Ces1g* and *Ces2a*, which are known to have triglyceride hydrolase functions, were also down-regulated in response to loss of *Gata4* (Lian et al. 2018). Future studies are needed to confirm the mechanisms underlying the phenotypes of Gata4LKO mice.

Previous GWASs have associated the *GATA4* gene and GATA4 binding with hyperlipidemia in humans (Asselbergs et al. 2012; Chou et al. 2022). Using GWAS databases, we found that SNPs with associations with HDL and LDL cholesterol levels in humans map within the GATA4 gene. However, functional studies are needed to validate the role of these variants in human metabolism.

Our study identified LXR as an important transcriptional partner for GATA4 in the liver. GATA4, HNF4A, and LXR were also shown to participate in the regulation of *ABCG5* and *ABCG8* in HepG2 cells (Sumi et al. 2007; Back et al. 2013). Our data reveal that GATA4 and LXR collaborate at many loci across the genome and that the overlap in their binding increases when LXR is activated. LXR appears to require the presence of GATA4 to fully activate its shared targets. Genes with enhancers that bound both GATA4 and LXR were more likely to be down-regulated in Gata4LKO livers, indicating the functional importance of this cooperation. Moreover, loss of GATA4 interfered with the up-regulation of some LXR target genes in response to LXR agonist treatment. However, future studies are needed to explore the mechanism of this cooperation and the metabolic roles of the LXR–GATA4 axis, especially in cholesterol efflux and triglyceride metabolism in physiology and pathologies such as NAFLD. In summary, hepatic GATA4 plays a central role in the transcriptional regulation of hepatic lipid metabolism in collaboration with LXR.

Materials and methods

Mice

C57BL/6J mice from Jax Laboratories (strain 000664) were used as wild-type mice in initial ATAC-seq and RNA-seq screens. Gata4-floxed/floxed mice were previously described (Watt et al. 2004) and were obtained from Jax Laboratories (strain 008194) and maintained on a mixed 129/C57BL/6 background. Gata4LKO mice were created by injecting AAV.TBG.PI.Cre.rBG (Addgene 107787-AAV8) or AAV.TBG.PI.Null.bGH (Addgene 105536-AAV8) for control at a concentration of 5×10^{11} genome copies per mouse at 8–10 wk of age. For the *Gata4* overexpression experiment, a Gateway system (Life Technologies) was used to recombine adeno pENTR-2B-Gata4 (Addgene plasmid 98615) and pAd/CMV/V5-DEST. Adenovirus particles were generated by transfection into 293A cells. Crude virus extracts were amplified, purified, and titered by Viraquest. Mice were injected with 4×10^8 pfu of pAd-CMV-GFP or pAd-CMV-Gata4. One week after the injection, mice were euthanized after 6 h of fasting.

High-sucrose (HS) diet (69% sucrose, 10% fat; D07042201) and RD Western diet (40% calories from fat, 0.2% cholesterol; D12079B) were obtained from Research Diets. In fasting and refeeding experiments, the refed group was fasted for 12 h starting at 9:00 a.m. and refed for 12 h with HS diet starting at 9:00 p.m. The fasted group was fasted for 12 h starting at 9:00 p.m. Both groups had access to water throughout and were sacrificed at 9:00 a.m. to 10:00 a.m. the following day. In other experiments, mice started fasting at 8:00 a.m. to 9:00 a.m. and were sacrificed at 2:00 p.m. to 3:00 p.m. Mice had ad libitum access to chow unless another diet was specified and were housed in pathogen-free facilities maintained on 12-h light/dark cycles at 22°C. The mouse studies were approved by the University of California at Los Angeles (UCLA) Chancellor's Animal Research Committee.

ATAC-seq sample preparation and sequencing

ATAC-seq from tissue was conducted as described previously (Bideyan et al. 2022). In summary, fresh tissue was homogenized in nuclear isolation buffer (20 mM Tris-HCl, 50 mM EDTA, 5 mM spermidine, 0.15 mM spermine, 0.1% mercaptoethanol, 40% glycerol, 1 mM EGTA, 60 mM KCl, 1% Igepal at pH 7.5) and filtered with 40-µm filters. Samples were centrifuged and resuspended with cold resuspension buffer (RSB; 10 mM Tris-HCl, 10 mM NaCl, 3 mM $MgCl_2$ at pH 7.4). Transposase reaction was performed on ~50,000 nuclei from these samples, DNA was purified using a Qiagen MinElute kit, and libraries were prepared as described (Buenrostro et al. 2015). Size selection was done with AMPure XP magnetic beads. Libraries were quantified using a NEBNext library quantification kit for Illumina and were sequenced on an Illumina HiSeq 4000 by single-end 50-bp sequencing.

RNA-seq sample preparation and sequencing

RNA was extracted from frozen tissue using TRIzol (Invitrogen) and a Qiagen RNeasy mini kit. The libraries were made with a KAPA stranded kit with mRNA capture. Libraries were sequenced on an Illumina HiSeq 3000 by single-end 50-bp or paired-end 50-bp sequencing on a Novaseq SP 100.

Chromatin immunoprecipitation

Chromatin was prepared from frozen tissue using truChIP chromatin shearing tissue kit (Covaris). Chromatin was sheared using a Diagenode Bioruptor Pico for 30 sec on/30 sec off for 10 cycles in

SDS lysis buffer (1% SDS, 10 mM EDTA at pH 8.1, 50 mM Tris-HCl at pH 8.1) supplemented with protease inhibitor cocktail. Input was decross-linked overnight at 65°C in elution buffer (0.1 M $NaHCO_3$, 0.1% SDS, 200 mM NaCl) followed by treatment with 0.125 ug/mL RNase A (Thermo Scientific) and 0.1 mg/mL Proteinase K. Chromatin was purified using QIAquick PCR purification kit and quantified using Qubit (dsDNA HS). Protein A Dynabeads (Invitrogen) were preincubated with 4 µg of H3K27ac (Abcam ab4729) or rabbit anti-GATA4 antibody (Fortis Life Sciences A303-503A) in ChIP dilution buffer (0.01% SDS, 1.1% Triton X-100, 1 mM EDTA at pH 8.1, 16.7 mM Tris-HCl at pH 8.1, 167 mM NaCl plus proteinase inhibitor) for 1.5 h at room temperature. Seven micrograms to 10 µg of chromatin was incubated overnight with the corresponding antibody-bound beads with rotation for immunoprecipitation (IP). IP samples were washed with low-salt wash buffer (0.1% SDS, 1% Triton X-100, 2 mM EDTA at pH 8.1, 20 mM Tris-HCl at pH 8.1, 150 mM NaCl) followed by high-salt wash buffer (0.1% SDS, 1% Triton X-100, 2 mM EDTA at pH 8.1, 20 mM Tris-HCl at pH 8.1, 500 mM NaCl), LiCl wash buffer (250 mM LiCl, 1% deoxycholic acid, 1 mM EDTA at pH 8.1, 10 mM Tris-HCl at pH 8.1, 1% Igepal), and finally two washes with TE buffer (1 mM EDTA at pH 8.1, 10 mM Tris-HCl at pH 8.1) (Ferrari et al. 2017). IP samples were decross-linked and purified as described for the input above. GATA4 ChIP samples and inputs were assessed using qPCR. Previously defined Gata4-negative genomic regions (Fx-neg and Alb-neg) (Zheng et al. 2013) were used to normalize across all samples in the qPCR calculation. Values represent the average fold change over the negative regions. Primer sequences for targets and controls are in Supplemental Table S2. H3K27ac ChIP samples and inputs were assessed by single-end 50-bp sequencing in a HiSeq 3000.

High-throughput sequencing data processing

For RNA-seq, reads were aligned to the mm9 or m10 genome using STAR (Dobin et al. 2013). DESeq2 and Seqmonk were used to generate normalized counts or reads per kilobase of transcript per million mapped reads (RPKM). DESeq2 was used to identify differentially expressed genes with an FDR < 0.05 cutoff. For ATAC-seq and ChIP-seq, trimmed sequences were aligned to the mm9 using bowtie2 (Langmead and Salzberg 2012). Reads were filtered using SAMtools (Li et al. 2009). Peaks were called using MACS2, and consensus peaks were created using BedTools (Zhang et al. 2008). For ATAC-seq, peaks were quantitated across samples and normalized to million reads per sample and peak length (RPKM) using Seqmonk. Differentially accessible peaks were determined using EdgeR (Robinson et al. 2010). For ChIP-seq, peaks were quantitated, and differentially expressed peaks were selected using Diffbind (Ross-Innes et al. 2012). FDR of <0.05 was used to identify differentially accessible or enriched peaks.

Peaks were annotated to genes with nearest promoter via HOMER (Heinz et al. 2010). Replicates were merged using SAMtools. Bedgraphs were created using HOMER and visualized using IGV (Robinson et al. 2011). Peaks with a minimum of 10 counts were ranked based on the fold difference between the conditions. Ranked peaks were divided into bins, each containing ~1000 peaks, and known motif analysis was run for each bin using HOMER. The *P*-value for each motif across all bins was calculated. Highly similar motifs (>0.9 similarity score) were summarized by one motif, and motifs that were not differentially enriched were omitted from the heat map for simplicity. HOMER was used to identify the genomic regions in which the motifs were present.

High-throughput sequencing data analysis and visualization

Heat maps were created using the ClustVis web tool (Metsalu and Vilo 2015). Unit variance scaling was used except for Supplemental Figure S1, C and D. Bioplanet, Wikipathways, and KEGG from Enrichr; gene set enrichment analysis (GSEA); and integrated pathway analysis (IPA) software were used for pathway enrichment analysis (Subramanian et al. 2005; Chen et al. 2013). FDR of <0.05 was used for identifying differentially expressed genes. The genes were ranked based on fold change and *P*-value ($-\log_2$FC × $-\log_{10}P$-value) for GSEA. DeepTools2 was used through both Commandline and Galaxy to quantify and profile the signal intensity in the ATAC-seq and ChIP-seq samples across defined peak sets (Afgan et al. 2016; Ramírez et al. 2016). The BedTools window function with a 500-bp range was used to identify H3K27ac peaks near GATA4 and LXR ChIP-seq sites, and a 1-kb range was used to identify H3K4me1 and H3K4me3 peaks near GATA4 ChIP-seq sites.

Plasma and liver metabolic assays

Lipids were extracted from livers using the methods of Bligh and Dyer (1959). Total cholesterol and NEFAs were measured using commercially available TC and NEFA kits from WAKO, and triglycerides were measured using the TG kit from Sekisui Diagnostics for both plasma and liver lipid extracts. To resolve lipoprotein classes by fast protein liquid chromatography, plasma was injected into a Superose 6 10/300 (GE Healthcare Life Sciences) chromatography column, and sequential fractions (1–80) were collected for measurement of cholesterol by colorimetric assay (WAKO NC9138103).

Lipidomics

Our lipidomics experiments used direct infusion-tandem mass spectrometry and were performed on a SCIEX 5500 triple-quadrupole (QQQ) with a Shimadzu autosampler, a SelexION ion mobility device, and a Shimadzu LC. Species were quantified using the Sciex lipidyzer platform and Sciex and Avanti polar lipid standards.

Liver glycogen assay

Frozen liver samples were prepared as described previously (Priest et al. 2022) by precipitating proteins. A glycogen assay kit (Sigma-Aldrich) was used according to the manufacturer's instructions, and the measurements were normalized to protein content.

RT-qPCR

For gene expression analysis, TRIzol was used to isolate RNA from frozen tissue, and concentrations and quality were measured using Nanodrop. For eRNA analysis, RNA was extracted from frozen tissue using TRIzol (Invitrogen) and Qiagen RNeasy mini kit including DNase treatment according to the manufacturers' instructions. cDNA was made, and real-time RT-qPCR (Bio-Rad) and Applied Biosystems Quant Studio 6 Flex were used for RT-qPCR. Primers for gene expression are in Supplemental Table S3. Primers for positive and negative strands of eRNA were designed based on the liver GRO-seq data (GSE59486) using the IDT PrimerQuest design tool (Supplemental Table S4). Counts were normalized to the 36B4 expression from the same samples.

Western blotting

Proteins were isolated with radioimmunoprecipitation assay buffer (Boston BioProducts) as described previously (Priest et al. 2022). Samples were loaded onto Bis-Tris gels, and proteins were separated by electrophoresis and then transferred to polyvinylidene difluoride membranes. The membranes were blocked in 5% nonfat milk in phosphate-buffered saline (PBS). Rabbit anti-GATA4 antibody (Fortis Life Sciences A303-503A-M) and antiactin antibody (Sigma-Aldrich A2066) were used as the primary antibodies, and horseradish peroxidase-conjugated antirabbit IgG (Jackson Laboratory) was used as the secondary antibody. Signal was produced using Immobilon Forte Western HRP substrate (EMD Millipore). The Western blot was quantified using GelQuantNET software.

Histology

Tissues were fixed in 4% paraformaldehyde. Tissues were mounted in paraffin, and 10-μm sections were cut. Sections were stained with hematoxylin and eosin (H&E). Oil Red O staining was done as described previously (Mehlem et al. 2013). Tissues were fixed in Tissue-Tek O.C.T. compound (Sigma 4583) on dry ice. Five-micrometer sections were cut using a Microm HM 505 E cryostat and placed on glass slides. Oil Red O solution (~0.4%; Sigma 00625) was used for staining. A Zeiss Axioskop 2 plus bright-field light microscope was used to capture the images.

VLDL secretion assay

Six-hour-fasted mice were injected with 1.0 g of poloxamer-407 (10% [w/v] in saline; Sigma-Aldrich 16758) per kilogram of body weight (https://www.protocols.io/view/hepatic-vldl-secretion-assay-izxcf7n). Blood samples were collected at 0-, 1-, 2-, 3-, and 4-h time points via retro-orbital bleeding and cardiac puncture for the final time point. Plasma was obtained by centrifuging blood at 2000*g* for 15 min. Plasma was assayed for lipids as described above.

LXR agonist treatment

Nine-week-old Gata4LKO and control mice, 1 wk after AAV injection, were gavaged with 40 mg/kg GW3965 prepared in canola oil (Collins et al. 2002) at 17 h and then again 8 h before sacrifice. Mice were 4-h-fasted at the time of killing. Dimethylsulfoxide in canola oil was used as vehicle control. Gene expression was determined via RT-PCR as described above.

Cell culture studies

Hepa1–6 cells were deprived of FBS, glucose, and glutamine in base Dulbecco's modified Eagle medium (DMEM) that was supplemented with or without 100 nM insulin for 8 h. RNA was extracted, and RT-PCR was used in assessing *Gata4* expression.

GWAS data

The SNPs and the Manhattan plot for the GATA4 loci for HDL and LDL traits were obtained from the Type 2 Diabetes Knowledge Portal on August 1, 2022. GATA4 loci were defined as the default LD block spanning chr8: 11,484,468–11,667,511 in the hg19 genome build.

Additional data sets

Gata4 expression throughout 24 h with and without fasting (GSE107787), GATA4 ChIP-seq (GSE49132), and LXR liver ChIP-seq data with and without agonist treatment (GSE35262)[33] were obtained from Gene Expression Omnibus (GEO). Peaks for H3K4me1 ChIP-seq (GSM722760) and H3K4me3 ChIP-seq (GSM722761) from murine livers and aggregate ChIP-seq data were obtained from the ChIP-Atlas website.

Data availability

RNA-seq (GSE212485) and ATAC-seq (GSE212483) of fasted and refed wild-type livers, RNA-seq (GSE212486) and H3K27ac ChIP-seq (GSE212484) of fasted and refed Gata4LKO and control livers, RNA-seq (GSE212487) of livers of Gata4LKO and control mice on Western diet, and RNA-seq (GSE218420) of livers of GW3965-treated or vehicle-treated Gata4LKO and control mice were deposited to the NCBI Gene Expression Omnibus under the SuperSeries accession number GSE212488.

Competing interest statement

The authors declare no competing interests.

Acknowledgments

We thank all members of the Tontonoz laboratory for technical support and valuable discussions. We thank the staff at the University of California at Los Angeles Technology Center for Genomics and Bioinformatics, the Broad Stem Cell Research Center, the Lipidomics Core, and the Translational Pathology Core Laboratory for their services and assistance. We thank the Sigrid Juselius and Instrumentarium Foundation for their postdoctoral mobility support for M.L.R. Funding for this project was provided by grants from the National Institutes of Health (HL136618, DK126779, and DK063491) to P.T.

Author contributions: L.B. and P.T. designed the study and wrote the manuscript. L.B., M.L.R., C.P., J.P.K., Y.G., and A.F. conducted the experiments. L.B., M.L.R., J.P.K., A.-C.F., and P.R. analyzed the data. S.G.T. and S.T.S. provided critical reagents and analysis methodology.

References

Afgan E, Baker D, van den Beek M, Blankenberg D, Bouvier D, Čech M, Chilton J, Clements D, Coraor N, Eberhard C, et al. 2016. The galaxy platform for accessible, reproducible and collaborative biomedical analyses: 2016 update. *Nucleic Acids Res* **44:** W3–W10. doi:10.1093/nar/gkw343

Arroyo N, Villamayor L, Díaz I, Carmona R, Ramos-Rodríguez M, Muñoz-Chápuli R, Pasquali L, Toscano MG, Martín F, Cano DA, et al. 2021. GATA4 induces liver fibrosis regression by deactivating hepatic stellate cells. *JCI Insight* **6:** e150059. doi:10.1172/jci.insight.150059

Asselbergs FW, Guo Y, van Iperen EPA, Sivapalaratnam S, Tragante V, Lanktree MB, Lange LA, Almoguera B, Appelman YE, Barnard J, et al. 2012. Large-scale gene-centric meta-analysis across 32 studies identifies multiple lipid loci. *Am J Hum Genet* **91:** 823–838. doi:10.1016/j.ajhg.2012.08.032

Back SS, Kim J, Choi D, Lee ES, Choi SY, Han K. 2013. Cooperative transcriptional activation of ATP-binding cassette sterol transporters ABCG5 and ABCG8 genes by nuclear receptors

including liver-X-receptor. *BMB Rep* **46:** 322–327. doi:10.5483/BMBRep.2013.46.6.246

Battle MA, Bondow BJ, Iverson MA, Adams SJ, Jandacek RJ, Tso P, Duncan SA. 2008. GATA4 is essential for jejunal function in mice. *Gastroenterology* **135:** 1676–1686.e1. doi:10.1053/j.gastro.2008.07.074

Bergeron F, Nadeau G, Viger RS. 2015. GATA4 knockdown in MA-10 Leydig cells identifies multiple target genes in the steroidogenic pathway. *Reproduction* **149:** 245–257. doi:10.1530/REP-14-0369

Bideyan L, Nagari R, Tontonoz P. 2021. Hepatic transcriptional responses to fasting and feeding. *Genes Dev* **35:** 635–657. doi:10.1101/gad.348340.121

Bideyan L, Fan W, Kaczor-Urbanowicz KE, Priest C, Casero D, Tontonoz P. 2022. Integrative analysis reveals multiple modes of LXR transcriptional regulation in liver. *Proc Natl Acad Sci* **119:** e2122683119. doi:10.1073/pnas.2122683119

Bligh EG, Dyer WJ. 1959. A rapid method of total lipid extraction and purification. *Can J Biochem Physiol* **37:** 911–917. doi:10.1139/y59-099

Boergesen M, Pedersen TÅ, Gross B, van Heeringen SJ, Hagenbeek D, Bindesbøll C, Caron S, Lalloyer F, Steffensen KR, Nebb HI, et al. 2012. Genome-wide profiling of liver X receptor, retinoid X receptor, and peroxisome proliferator-activated receptor α in mouse liver reveals extensive sharing of binding sites. *Mol Cell Biol* **32:** 852–867. doi:10.1128/MCB.06175-11

Buenrostro JD, Wu B, Chang HY, Greenleaf WJ. 2015. ATAC-seq: a method for assaying chromatin accessibility genome-wide. *Curr Protoc Mol Bio* **109:** 21.29.1–21.29.9. doi:10.1002/0471142727.mb2129s109

Chen EY, Tan CM, Kou Y, Duan Q, Wang Z, Meirelles GV, Clark NR, Ma'ayan A. 2013. Enrichr: interactive and collaborative HTML5 gene list enrichment analysis tool. *BMC Bioinformatics* **14:** 128. doi:10.1186/1471-2105-14-128

Chou W-C, Chen W-T, Shen C-Y. 2022. A common variant in 11q23.3 associated with hyperlipidemia is mediated by the binding and regulation of GATA4. *NPJ Genom Med* **7:** 1–10. doi:10.1038/s41525-021-00279-5

Collins JL, Fivush AM, Watson MA, Galardi CM, Lewis MC, Moore LB, Parks DJ, Wilson JG, Tippin TK, Binz JG, et al. 2002. Identification of a nonsteroidal liver X receptor agonist through parallel array synthesis of tertiary amines. *J Med Chem* **45:** 1963–1966. doi:10.1021/jm0255116

Creyghton MP, Cheng AW, Welstead GG, Kooistra T, Carey BW, Steine EJ, Hanna J, Lodato MA, Frampton GM, Sharp PA, et al. 2010. Histone H3K27ac separates active from poised enhancers and predicts developmental state. *Proc Natl Acad Sci* **107:** 21931–21936. doi:10.1073/pnas.1016071107

Ding L, Cai M, Chen L, Yan H, Lu S, Pang S, Yan B. 2021. Identification and functional study of GATA4 gene regulatory variants in type 2 diabetes mellitus. *BMC Endocr Disord* **21:** 73. doi:10.1186/s12902-021-00739-0

Dobin A, Davis CA, Schlesinger F, Drenkow J, Zaleski C, Jha S, Batut P, Chaisson M, Gingeras TR. 2013. STAR: ultrafast universal RNA-seq aligner. *Bioinformatics* **29:** 15–21. doi:10.1093/bioinformatics/bts635

Duell PB, Welty FK, Miller M, Chait A, Hammond G, Ahmad Z, Cohen DE, Horton JD, Pressman GS, Toth PP, et al. 2022. Nonalcoholic fatty liver disease and cardiovascular risk: a scientific statement from the American heart association. *Arterioscler Thromb Vasc Biol* **42:** e168–e185. doi:10.1161/ATV.0000000000000153

Enane FO, Shuen WH, Gu X, Quteba E, Przychodzen B, Makishima H, Bodo J, Ng J, Chee CL, Ba R, et al. 2017. GATA4 loss of function in liver cancer impedes precursor to hepatocyte transition. *J Clin Invest* **127:** 3527–3542. doi:10.1172/JCI93488

Ferrari A, Longo R, Fiorino E, Silva R, Mitro N, Cermenati G, Gilardi F, Desvergne B, Andolfo A, Magagnotti C, et al. 2017. HDAC3 is a molecular brake of the metabolic switch supporting white adipose tissue browning. *Nat Commun* **8:** 93. doi:10.1038/s41467-017-00182-7

Francis GA. 2016. High-density lipoproteins: metabolism and protective roles against atherosclerosis. In *Biochemistry of lipids, lipoproteins and membranes*, 2nd ed (ed. Ridgway ND, McLeod RS), pp. 437–457. Elsevier, Boston.

Goldstein JL, Brown MS. 2015. A century of cholesterol and coronaries: from plaques to genes to statins. *Cell* **161:** 161–172. doi:10.1016/j.cell.2015.01.036

He A, Gu F, Hu Y, Ma Q, Yi Ye L, Akiyama JA, Visel A, Pennacchio LA, Pu WT. 2014. Dynamic GATA4 enhancers shape the chromatin landscape central to heart development and disease. *Nat Commun* **5:** 4907. doi:10.1038/ncomms5907

Heinz S, Benner C, Spann N, Bertolino E, Lin YC, Laslo P, Cheng JX, Murre C, Singh H, Glass CK. 2010. Simple combinations of lineage-determining transcription factors prime *cis*-regulatory elements required for macrophage and B cell identities. *Mol Cell* **38:** 576–589. doi:10.1016/j.molcel.2010.05.004

Joseph SB, Laffitte BA, Patel PH, Watson MA, Matsukuma KE, Walczak R, Collins JL, Osborne TF, Tontonoz P. 2002. Direct and indirect mechanisms for regulation of fatty acid synthase gene expression by liver X receptors. *J Biol Chem* **277:** 11019–11025. doi:10.1074/jbc.M111041200

Kinouchi K, Magnan C, Ceglia N, Liu Y, Cervantes M, Pastore N, Huynh T, Ballabio A, Baldi P, Masri S, et al. 2018. Fasting imparts a switch to alternative daily pathways in liver and muscle. *Cell Rep* **25:** 3299–3314.e6. doi:10.1016/j.celrep.2018.11.077

Lamina C, Coassin S, Illig T, Kronenberg F. 2011. Look beyond one's own nose: combination of information from publicly available sources reveals an association of GATA4 polymorphisms with plasma triglycerides. *Atherosclerosis* **219:** 698–703. doi:10.1016/j.atherosclerosis.2011.08.044

Langmead B, Salzberg SL. 2012. Fast gapped-read alignment with Bowtie 2. *Nat Methods* **9:** 357–359. doi:10.1038/nmeth.1923

Lentjes MH, Niessen HE, Akiyama Y, de Bruïne AP, Melotte V, van Engeland M. 2016. The emerging role of GATA transcription factors in development and disease. *Expert Rev Mol Med* **18:** e3. doi:10.1017/erm.2016.2

Li H, Handsaker B, Wysoker A, Fennell T, Ruan J, Homer N, Marth G, Abecasis G, Durbin R, 1000 Genome Project Data Processing Subgroup. 2009. The sequence alignment/map format and SAMtools. *Bioinformatics* **25:** 2078–2079. doi:10.1093/bioinformatics/btp352

Lian J, Nelson R, Lehner R. 2018. Carboxylesterases in lipid metabolism: from mouse to human. *Protein Cell* **9:** 178–195. doi:10.1007/s13238-017-0437-z

Liang G, Yang J, Horton JD, Hammer RE, Goldstein JL, Brown MS. 2002. Diminished hepatic response to fasting/refeeding and liver X receptor agonists in mice with selective deficiency of sterol regulatory element-binding protein-1c. *J Biol Chem* **277:** 9520–9528. doi:10.1074/jbc.M111421200

Mehlem A, Hagberg CE, Muhl L, Eriksson U, Falkevall A. 2013. Imaging of neutral lipids by Oil Red O for analyzing the metabolic status in health and disease. *Nat Protoc* **8:** 1149–1154. doi:10.1038/nprot.2013.055

Metsalu T, Vilo J. 2015. ClustVis: a web tool for visualizing clustering of multivariate data using principal component analysis and heatmap. *Nucleic Acids Res* **43:** W566–W570. doi:10.1093/nar/gkv468

Molkentin JD, Lin Q, Duncan SA, Olson EN. 1997. Requirement of the transcription factor GATA4 for heart tube formation and ventral morphogenesis. *Genes Dev* **11:** 1061–1072. doi:10.1101/gad.11.8.1061

Oka T, Maillet M, Watt AJ, Schwartz RJ, Aronow BJ, Duncan SA, Molkentin JD. 2006. Cardiac-specific deletion of *Gata4* reveals its requirement for hypertrophy, compensation, and myocyte viability. *Circ Res* **98:** 837–845. doi:10.1161/01.RES.0000215985.18538.c4

Patankar JV, Chandak PG, Obrowsky S, Pfeifer T, Diwoky C, Uellen A, Sattler W, Stollberger R, Hoefler G, Heinemann A, et al. 2011. Loss of intestinal GATA4 prevents diet-induced obesity and promotes insulin sensitivity in mice. *Am J Physiol Endocrinol Metab* **300:** E478–E488. doi:10.1152/ajpendo.00457.2010

Priest C, Nagari RT, Bideyan L, Lee SD, Nguyen A, Xiao X, Tontonoz P. 2022. Brap regulates liver morphology and hepatocyte turnover via modulation of the Hippo pathway. *Proc Natl Acad Sci* **119:** e2201859119. doi:10.1073/pnas.2201859119

Ramírez F, Ryan DP, Grüning B, Bhardwaj V, Kilpert F, Richter AS, Heyne S, Dündar F, Manke T. 2016. Deeptools2: a next generation web server for deep-sequencing data analysis. *Nucleic Acids Res* **44:** W160–W165. doi:10.1093/nar/gkw257

Repa JJ, Liang G, Ou J, Bashmakov Y, Lobaccaro J-MA, Shimomura I, Shan B, Brown MS, Goldstein JL, Mangelsdorf DJ. 2000a. Regulation of mouse sterol regulatory element-binding protein-1c gene (SREBP-1c) by oxysterol receptors, LXRα and LXRβ. *Genes Dev* **14:** 2819–2830. doi:10.1101/gad.844900

Repa JJ, Turley SD, Lobaccaro J-MA, Medina J, Li L, Lustig K, Shan B, Heyman RA, Dietschy JM, Mangelsdorf DJ. 2000b. Regulation of absorption and ABC1-mediated efflux of cholesterol by RXR heterodimers. *Science* **289:** 1524–1529. doi:10.1126/science.289.5484.1524

Repa JJ, Berge KE, Pomajzl C, Richardson JA, Hobbs H, Mangelsdorf DJ. 2002. Regulation of ATP-binding cassette sterol transporters ABCG5 and ABCG8 by the liver X receptors α and β. *J Biol Chem* **277:** 18793–18800. doi:10.1074/jbc.M109927200

Robinson MD, McCarthy DJ, Smyth GK. 2010. Edger: a Bioconductor package for differential expression analysis of digital gene expression data. *Bioinformatics* **26:** 139–140. doi:10.1093/bioinformatics/btp616

Robinson JT, Thorvaldsdóttir H, Winckler W, Guttman M, Lander ES, Getz G, Mesirov JP. 2011. Integrative genomics viewer. *Nat Biotechnol* **29:** 24–26. doi:10.1038/nbt.1754

Romano O, Miccio A. 2020. GATA factor transcriptional activity: insights from genome-wide binding profiles. *IUBMB Life* **72:** 10–26. doi:10.1002/iub.2169

Ross-Innes CS, Stark R, Teschendorff AE, Holmes KA, Ali HR, Dunning MJ, Brown GD, Gojis O, Ellis IO, Green AR, et al. 2012. Differential oestrogen receptor binding is associated with clinical outcome in breast cancer. *Nature* **481:** 389–393. doi:10.1038/nature10730

Rui L. 2014. Energy metabolism in the liver. *Compr Physiol* **4:** 177–197. doi:10.1002/cphy.c130024

Schrade A, Kyrönlahti A, Akinrinade O, Pihlajoki M, Häkkinen M, Fischer S, Alastalo T-P, Velagapudi V, Toppari J, Wilson DB, et al. 2015. GATA4 is a key regulator of steroidogenesis and glycolysis in mouse Leydig cells. *Endocrinology* **156:** 1860–1872. doi:10.1210/en.2014-1931

Subramanian A, Tamayo P, Mootha VK, Mukherjee S, Ebert BL, Gillette MA, Paulovich A, Pomeroy SL, Golub TR, Lander ES, et al. 2005. Gene set enrichment analysis: a knowledge-based approach for interpreting genome-wide expression profiles. *Proc Natl Acad Sci* **102:** 15545–15550. doi:10.1073/pnas.0506580102

Sumi K, Tanaka T, Uchida A, Magoori K, Urashima Y, Ohashi R, Ohguchi H, Okamura M, Kudo H, Daigo K, et al. 2007. Cooperative interaction between hepatocyte nuclear factor 4α and GATA transcription factors regulates ATP-binding cassette sterol transporters ABCG5 and ABCG8. *Mol Cell Biol* **27:** 4248–4260. doi:10.1128/MCB.01894-06

Venkateswaran A, Laffitte BA, Joseph SB, Mak PA, Wilpitz DC, Edwards PA, Tontonoz P. 2000. Control of cellular cholesterol efflux by the nuclear oxysterol receptor LXRα. *Proc Natl Acad Sci* **97:** 12097–12102. doi:10.1073/pnas.200367697

Watt AJ, Battle MA, Li J, Duncan SA. 2004. GATA4 is essential for formation of the proepicardium and regulates cardiogenesis. *Proc Natl Acad Sci* **101:** 12573–12578. doi:10.1073/pnas.0400752101

Watt AJ, Zhao R, Li J, Duncan SA. 2007. Development of the mammalian liver and ventral pancreas is dependent on GATA4. *BMC Dev Biol* **7:** 37. doi:10.1186/1471-213X-7-37

Winkler M, Staniczek T, Kürschner SW, Schmid CD, Schönhaber H, Cordero J, Kessler L, Mathes A, Sticht C, Neßling M, et al. 2021. Endothelial GATA4 controls liver fibrosis and regeneration by preventing a pathogenic switch in angiocrine signaling. *J Hepatol* **74:** 380–393. doi:10.1016/j.jhep.2020.08.033

Yang T, Espenshade PJ, Wright ME, Yabe D, Gong Y, Aebersold R, Goldstein JL, Brown MS. 2002. Crucial step in cholesterol homeostasis: sterols promote binding of SCAP to INSIG-1, a membrane protein that facilitates retention of SREBPs in ER. *Cell* **110:** 489–500. doi:10.1016/S0092-8674(02)00872-3

Zhang Y, Liu T, Meyer CA, Eeckhoute J, Johnson DS, Bernstein BE, Nusbaum C, Myers RM, Brown M, Li W, et al. 2008. Model-based analysis of ChIP-seq (MACS). *Genome Biol* **9:** R137. doi:10.1186/gb-2008-9-9-r137

Zheng R, Rebolledo-Jaramillo B, Zong Y, Wang L, Russo P, Hancock W, Stanger BZ, Hardison RC, Blobel GA. 2013. Function of GATA factors in the adult mouse liver. *PLoS One* **8:** e83723. doi:10.1371/journal.pone.0083723